Liquid Crystals
Publication details, including instructions for authors and subscription information:
http://www.informaworld.com/smpp/title~content=t713926090

Topological point defects in liquid crystalline polymers

John Hobdell[a]; Alan Windle[a]
[a] Department of Materials Science and Metallurgy, Cambridge University, Cambridge, England

To cite this Article Hobdell, John and Windle, Alan(1995) 'Topological point defects in liquid crystalline polymers', Liquid Crystals, 19: 4, 401 — 407
To link to this Article: DOI: 10.1080/02678299508031999
URL: http://dx.doi.org/10.1080/02678299508031999

LIQUID CRYSTALS, 1995, VOL. 19, NO. 4, 401–407

Topological point defects in liquid crystalline polymers

by JOHN HOBDELL and ALAN WINDLE*

Department of Materials Science and Metallurgy, Pembroke Street,
Cambridge University, Cambridge CB2 3QZ, England

(*Received 21 January 1995; accepted 13 April 1995*)

The full range of point defects of the type described by Poincaré is defined in terms of the disclination loop which would transform them into a monodomain. Calculations of energy of the points as a function of the defining angle, α, give the relative contributions of the splay, twist and bend components. Defects observed on fracture surfaces of a quenched liquid crystalline polymer are consistent with the point geometry predicted to have minimum splay distortion, and thus accountable for in terms of the high splay elastic constant characteristic of the polymeric nematic state.

1. Introduction

In 1886, just two years before Reinitzer [1] saw iridescent colours in esters of cholesterol which pointed to their liquid crystallinity, Poincaré [2] derived equations for point singularities in vector fields. His work was later summarized by Nabarro [3] who related it to observations of point defects in liquid crystals.

Frank's equation [4] for the free energy density of a distortion field in liquid crystals may be used to calculate the energy associated with possible point defects. Energies are expressed in terms of the three elastic constants of orientational distortion: namely splay, twist and bend. In liquid crystalline polymers, splay distortion is energetically unfavourable compared to twist and bend [5] and this difference will influence the configuration of the point defects which are most stable and thus likely to be observed.

The work reported in this paper involves the calculation of distortion energies for Poincaré point singularities with the graphical illustration of representative examples. It also exploits the availability of thermotropic liquid crystalline random copolymers [6] which provide a mesogenic medium in which melt defect structures can be quenched to a glass and examined by fractography. The crystallinity which does occur has virtually no effect on the microstructure, while the ability to examine bulk samples by fractography or sectioning side-steps the difficulty due to surface effects encountered in the observation of thin, molten specimens, as is necessary for conventional liquid crystals.

* Author for correspondence.

2. Point defects

It is possible to define a *topological charge* for a point singularity in a vector field as

$$N = \frac{1}{4\pi} \oint \mathbf{n} \left[\frac{\partial \mathbf{n}}{\partial \theta} \frac{\partial \mathbf{n}}{\partial \varphi} \right] \mathrm{d}\theta \, \mathrm{d}\varphi \qquad (1)$$

where θ and φ are arbitrary coordinates on the surface σ, and $\mathbf{n}$ is the vector field [7]; this topological invariant was first derived by Kléman [8]. In a nematic liquid crystalline material, the director field can be described by a vector field with the proviso that $\mathbf{n} = -\mathbf{n}$. Hence the topological charge may be either positive or negative depending on the choice of direction for the vectors representing the director field. Since this choice is arbitrary, it only makes sense to refer to the magnitude of the topological charge and not the sign. In true vector fields, this sign refers to whether the singularity is a source or a sink. The point singularities which Poincaré described all have a topological charge of magnitude one. Higher order points are mathematically possible, but are not considered further here. In addition, all of Poincaré's points have a special axis and a special plane. For the geometries considered here, the special plane is a mirror plane coincident with the x–y plane and the special axis is a rotational symmetry axis parallel to z.

Poincaré derived his points from a vector field of the form

$$\begin{aligned} n_x &= a_1 x + b_1 y + c_1 z, \\ n_y &= a_2 x + b_2 y + c_2 z, \\ n_z &= a_3 x + b_3 y + c_3 z. \end{aligned} \qquad (2)$$

0267–8292/95 $10·00

Table 1. Poincaré's classification of the various point singularities in vector fields depended on the eigenvalues found from equation (3). This table summarizes his classification and relates it to the characteristic angle, α, used here to provide a continuous variable against which distortion energies for the various configurations are plotted.

Point	α	λ_1	λ_2	λ_3
Noeud	0°	Real, positive	Real, positive	Real, positive
Foyer	$0° < \alpha < 90°$	Real, positive	Complex conjugates (real part positive)	
Centre	90°	Real, positive	Imaginary	Imaginary
Col-foyer	$90° < \alpha < 180°$	Real, positive	Complex conjugates (real part negative)	
Col	180°	Real, positive	Real, negative	Real, negative

He distinguished various possibilities by considering the eigenvalues found from

$$\begin{vmatrix} a_1 - \lambda & b_1 & c_1 \\ a_2 & b_2 - \lambda & c_2 \\ a_3 & b_3 & c_3 - \lambda \end{vmatrix} = 0 \qquad (3)$$

and used the nature of the roots, as listed in table 1, as a basis for classification. He also chose a simple algebraic example to illustrate each class, naming them *noeud*, *foyer*, *centre*, *col-foyer* and *col*. These French terms translate as knot, focus, centre, saddle-focus and saddle, although modern Russian literature refers to a *noeud* as a hedgehog and a *col* as a hyperbolic hedgehog, with possibly some descriptive advantage.

2.1. *Visualizing points*

Computer graphics programs have been written to aid in the visualization of Poincaré's points, the vector field being represented by an appropriate selection of streamlines. Each streamline is traced from a chosen starting point in accord with equation (2). A representative sample of the possible configurations is drawn in figure 1. In addition to the three-dimensional visualization of each point, sections both on the special plane and through the special axis are represented in figure 1 using the 'nail convention'.

2.2. *Examples of points*

The limiting cases of the Poincaré range are the *noeud* (hedgehog) and the *col* (hyperbolic hedgehog). The *noeud* has a radiating field with spherical symmetry. It is analogous to the electric field around an isolated point charge. The *col* exhibits the phenomenon of splay–splay compensation [5]. On the special plane, the splay distortion is cancelled out, since it splays away from the origin in the plane and splays towards the origin perpendicular to the plane. This reduction in splay energy in the *col* type point defect is emphasized by Press and Arrott [9] for the case of nematic droplets. This singularity is analogous to the flow field produced when two fluid jets impinge on each other.

2.3. *Classifying points*

Poincaré's five classes of point should not belie the fact that there is a continuous variation in configuration between the limits of the *noeud* and the *col*, there being no topological distinction between the classes. It is helpful, therefore, to consider a description in terms of a single smoothly changing variable. Such a variable can be found by considering the nature of the disclination loop, lying on the special plane of the point (normal to z figure 1), which would represent the topological transformation of the point into a monodomain.

Such loops, of ideal form, have the property that the Ω vector (the axis of rotational distortion) maintains a constant angular relationship with the disclination line as it curves around the loop. It can have any angle with respect to the disclination line. They have been termed type II loops [10] to distinguish them from type I in which the Ω vector is invariant and which shrink to self-annihilation leaving a monodomain.

Figure 2 is an example of how the angle between the Ω vector and the disclination line defines the geometric nature of the disclination. In each figure, the line is considered to be coming out of the page and a circuit around the line is shown in a right-handed sense. Following the circuit around, the orientation of the directors, shown as thick lines, changes by 180°. The axis about which the directors rotate, which in each case has a different orientation with respect to the disclination line (see caption), is the Ω vector. For a type II loop where the rotation vector, $\underline{\Omega}$, is at all points anti-parallel to the disclination line, the line is an $s = -\frac{1}{2}$ wedge (see figure 2(*b*)). The full loop is sketched in figure 3 and is an example of a tangential loop [10] with the rotation vector, $\underline{\Omega}$, parallel to the line at all points around the loop. The loop effectively separates a *col* type field, outside its circumference, from a monodomain within the loop. If the loop

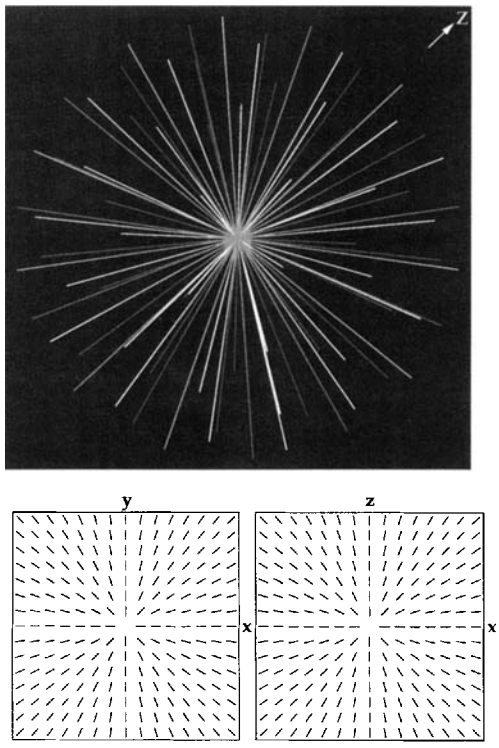

Figure 1 (*a*)

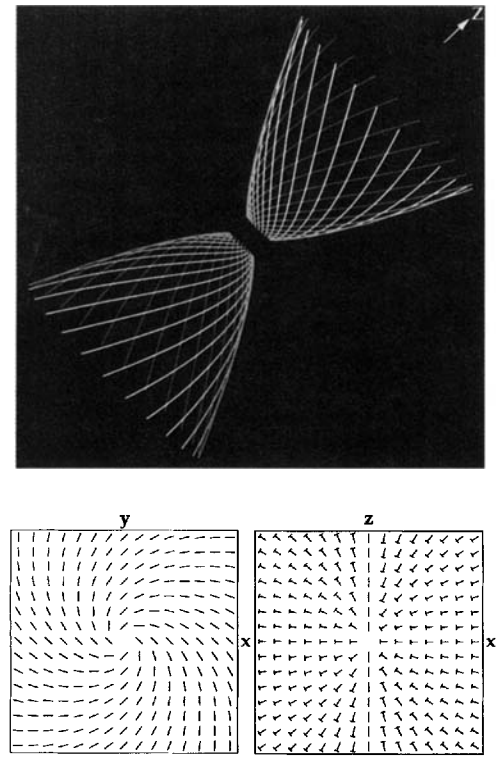

Figure 1 (*b*)

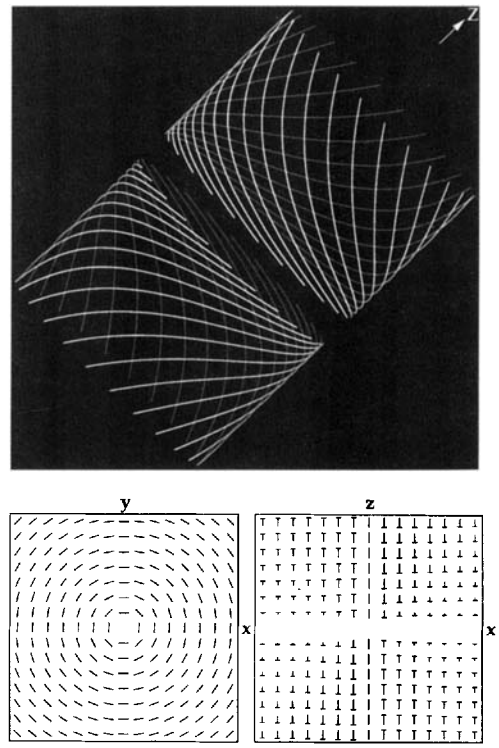

Figure 1 (*c*)

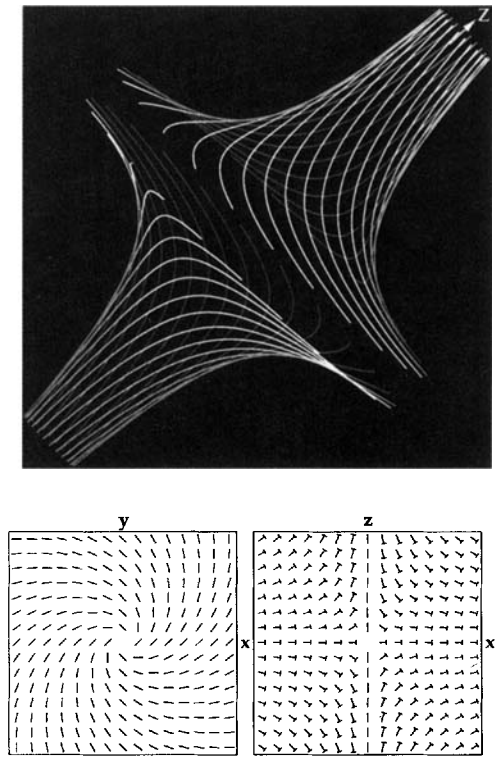

Figure 1 (*d*)

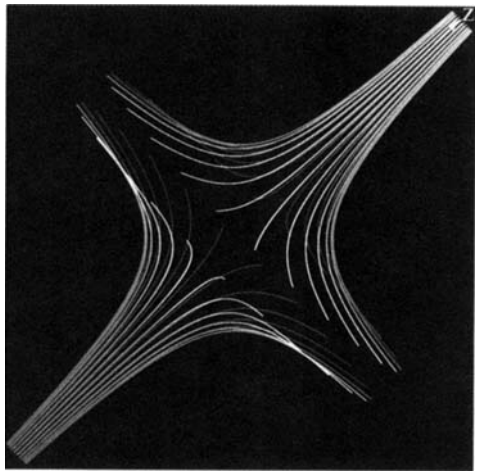

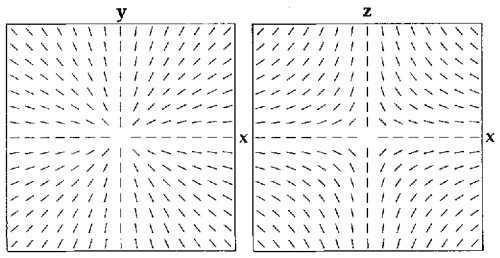

Figure 1 (*e*)

Figure 1. A representative sample of the possible configurations of the point singularities with unit topological charge described and classified by Henri Poincaré. For each case, an appropriate set of streamlines is plotted with the aid of computer graphics and 'nail diagrams' for two orthogonal sections through the points are given. The nail representation involves 'T' shaped objects with the cross of the 'T' representing the end of the vector further away from the observer and the length of the other line representing the component of the vector in the plane of the page. Nails with no cross line are exactly in the plane of the page. (*a*) A *noeud* or hedgehog point given by the defining equation $n_x = x/r$, $n_y = y/r$, $n_z = z/r$. (*b*) A *foyer* type point given by the defining equation $n_x = (x + y)/\sqrt{(2)}r$, $n_y = (-x + y)/\sqrt{(2)}r$, $n_z = z/r$. (*c*) A *centre* point given by the defining equation $n_x = y/r$, $n_y = -x/r$, $n_z = z/r$. (*d*) A *col-foyer* type point given by the defining equation $n_x = (-x + y)/\sqrt{(2)}r$, $n_y = (-x - y)/\sqrt{(2)}r$, $n_z = z/r$. (*e*) A *col* or hyperbolic hedgehog point given by the defining equation $n_x = -x/r$, $n_y = -y/r$, $n_z = z/r$. In each case, the vector fields are normalized to be of unit magnitude everywhere by the factor $r = \sqrt{(x^2 + y^2 + z^2)}$.

shrinks to a point, it will generate a *col* (hyperbolic hedgehog) point singularity. The other case of a tangential loop occurs when the rotation vector is at all points parallel to the direction of the disclination line. If such a loop were to shrink, a *noeud* (hedgehog) point singularity would be the result. In the particular case of a radial [10] loop, where the rotation vector is everywhere perpendicular to the direction of the disclination line, and in the plane of the loop, the loop would shrink to give a *centre* type point.

As such type II loops effectively define a point defect, it is possible to classify a point singularity simply in terms of the angle between the Ω vector and the line of the parent loop, the characteristic angle, α. It follows that the points considered above, *noeud* ($\alpha = 0°$), *centre* ($\alpha = 90°$) and *col* ($\alpha = 180°$) are but examples from a continuous range of point configurations, the range between *noeud* and *centre* ($0° < \alpha < 90°$) being known as *foyers*, and between *centre* and *col* ($90° < \alpha < 180°$) as *col-foyers*. The specific examples of *foyer* and *col-foyer* type points visualized in figure 1 can be considered as the result of shrinking a loop of disclination line in which the Ω vector lies at 45° to the direction of the line ($\alpha = 45°$) for the *foyer* example (see figure 1 (*b*)), and at 135° to the direction of the line ($\alpha = 135°$) for the *col-foyer* example (see figure 1 (*d*)). Equations (4), written in terms of α, thus define the full range (see table 1), which includes the specific examples of figure 1.

$$n_x = \frac{x\cos\alpha + y\sin\alpha}{r},$$
$$n_y = \frac{-x\sin\alpha + y\cos\alpha}{r}, \qquad (4)$$
$$n_z = \frac{z}{r} \quad \text{where} \quad r = (x^2 + y^2 + z^2)^{1/2}.$$

It is worth noting that the field lines at the special plane are always parallel to that plane, and follow equiangular spirals which intersect radii at the characteristic angle, α.

2.4. *Energies of points*

Frank's elasticity equation for the free energy associated with a distortion field may be integrated over a spherical volume around a point singularity to give a value for the elastic energy within a spherical volume of radius R. For simple cases, this integration may be performed analytically with relative ease. Dubois-Violette and Parodi [11] have derived the energy of a *noeud* (hedgehog) type point as

$$E_{\text{Noeud}} = 8\pi k_{11} R \qquad (5)$$

where k_{11} is the Frank splay constant, while Kurik and Lavrentovich [12] give the energy of a *col* (hyperbolic hedgehog) as

$$E_{\text{Col}} = 8\pi R\left(\frac{k_{11}}{5} + \frac{2k_{33}}{15}\right) \qquad (6)$$

where k_{33} is the Frank bend constant.

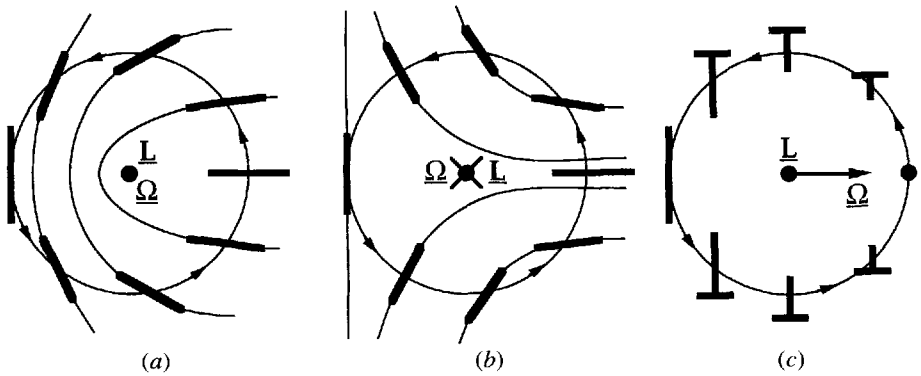

Figure 2. As one takes a clockwise circuit around each of the disclination lines shown coming out of the plane of the page, the orientation of the director changes by 180°. In (*a*) the axis of rotation, or Ω vector, is parallel to the line resulting in a $+\frac{1}{2}$ wedge disclination. In (*b*) the Ω vector is antiparallel to the direction of the line resulting in a $-\frac{1}{2}$ wedge disclination. In (*c*) the Ω vector is perpendicular to the line resulting in a strength $\frac{1}{2}$ twist disclination line. In general, the Ω vector can be at any angle to the disclination line when the line will have intermediate character.

In order to calculate the energies of the more complex point defects, a numerical approach has been introduced. The vector field surrounding the point is differentiated, using the REDUCE [13] program, to give the splay, twist and bend contributions to the free energy density as a function of the Cartesian coordinates. A simple numerical integration is performed by evaluating the free energy density at points on a three-dimensional array of cubic cells and multiplying by the volume of a cell, and then summing the values for all of the cells. By increasing the resolution of the array, the numerical integration converged to give agreement with the analytical values for the *noeud* and *col*. The convergence for a *noeud* is shown in figure 4. The numerically determined energies are given in table 2, based on an array of 100 linear divisions, for the *centre* (90°), the 45° *foyer* and the 135° *col-foyer* which are less analytically tractable.

The description of point configurations in terms of their transforming disclination loops gives a continuous variable, namely the characteristic angle, against which the splay, twist and bend energies can be plotted. Such a plot is shown in figure 5. The energies are expressed in units of kR, where k is the relevant elastic constant and R is the radius of integration, the curves give a quantitative indication of the total amount of each distortion which is present in each type of point defect.

It is interesting to note from figure 5 that the twist energy is zero for the *noeud* and *col*, rising to a maximum for the *centre*. Such behaviour is consistent with the fact that the *noeud* and *col* are the result of shrinking loops of wedge disclination which have no twist distortion, while the *centre* is the result of shrinking a loop of twist disclination. On the other hand, the splay energy, is a maximum for the *noeud* type point defect and decreases to a minimum at

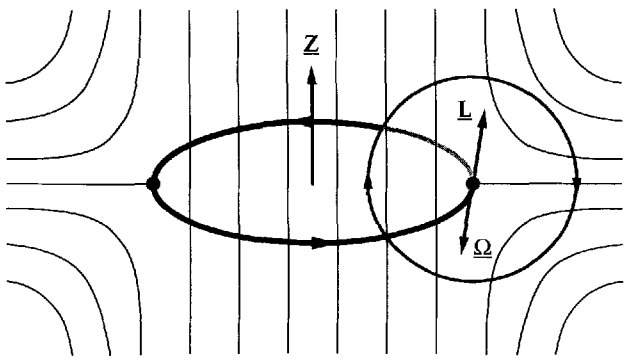

Figure 3. A loop of wedge disclination line L. The Ω vector is always at 180° to the line of the loop. The result is a cylindrically symmetric field which resembles a *col* or hyperbolic hedgehog when viewed on a scale much larger than that of the loop. A cross-section through the director field pattern is shown.

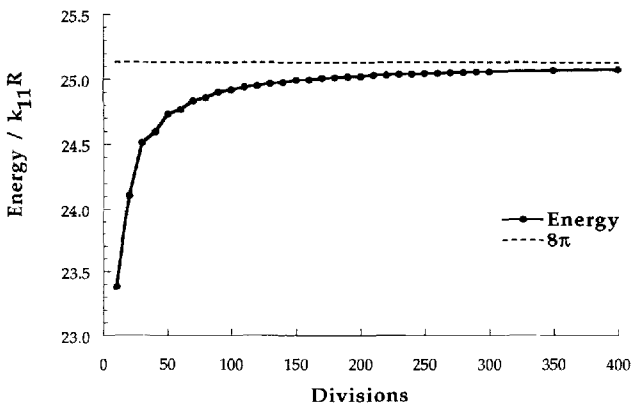

Figure 4. Plot showing the convergence of the numerical calculation of the energy of a *noeud* or hedgehog as a function of the number of divisions across the diameter of the integration sphere. The analytical value of 8π is shown for comparison.

Table 2. The splay, twist and bend energies associated with the examples of specific point defects shown in figure 1, as determined by the numerical method. In addition, the total elastic distortion energies are given for the widely considered case of equal elastic constants. Analytical values are published elsewhere for both the *noeud* and the *col*.

		Total energy for equal constants		Individual contributions to distortion energy		
Point	α	Numerical kR	Analytical kR	Splay $k_{11}R$	Twist $k_{22}R$	Bend $k_{33}R$
Noeud	0°	24·92	25·15	24·92	0·00	0·00
Foyer	45°	22·48	—	16·18	4·15	2·15
Centre	90°	16·61	—	3·31	8·31	4·99
Col-foyer	135°	10·74	—	2·07	4·15	4·52
Col	180°	8·31	8·37	4·95	0·00	3·36

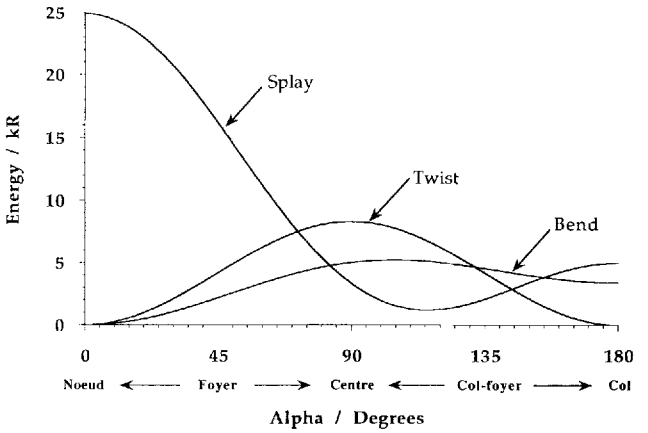

Figure 5. Plot of splay, twist and bend energies as a function of the characteristic angle, α, for a series of point defects as defined by equation (4).

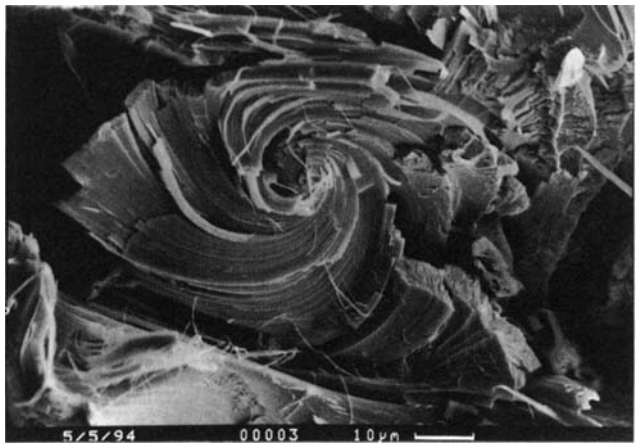

Figure 6. A fracture surface of a thermotropic main chain liquid crystalline polymer of molecular mass 5000. The polymer is a random copolyester of 75 per cent hydroxybenzoic acid and 25 per cent hydroxynaphthoic acid:

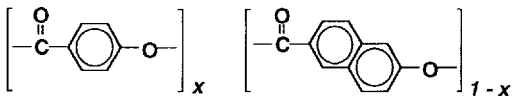

The director pattern, as revealed by the directional fissility, is compatible with an equatorial section through a point defect of the *col-foyer* type.

$\alpha = 115°$ (in the *col-foyer* range), before rising again towards the *col*. The significance of this minimum is that it would indicate the preferred structure when the splay constant is much higher than the other two, as is the case for polymeric nematics. The existence of such a minimum has been recorded in [14] in which liquid crystal defects are explored as observable analogues of strings and monopoles in cosmological fields. Calculations by Press and Arrott [9] have also shown that with a certain set of elastic constants, a twisted, cylindrically symmetrical point defect has a lower energy than the radially symmetric point. Much research into point defects in magnetization fields has been performed (for a review see [15]) and it is interesting to note that the point defects which could occur in these *vector* fields are the same as the point defects which could occur in *nematic* fields, but that in the vector case, the strength one points cannot decompose into loops of strength $\frac{1}{2}$ line, since such lines are disallowed.

3. Experimental observations

Point defects in the director pattern have been reported in small molecule liquid crystals by various workers. Williams *et al.* [16], observed *noeuds* and *cols* in capillary tubes treated to impose homeotropic boundary conditions at the walls of the tube. More recently, Melzer and Nabarro [17, 18] have attempted to produce *col-foyer* type points by treating the tube bore to give planar, but circumferential boundary conditions. Although they were not successful with this approach, they were able to stabilize a *col-foyer* type point defect by introducing planar, helical boundary conditions of opposite sense from each end of the tube. Point singularities have also been observed in nematic droplets. Laventovich and Terentjev [19] reported points in small molecule nematic droplets with character changing from *noeud* to *col* as the elastic constant for bend

increases on cooling towards the nematic–smectic phase transition temperature.

Part of the motivation for this analysis has been the observation of features, such as that shown in figure 6, on fracture surfaces of samples of a thermotropic liquid crystalline polymer which has been quenched from the nematic phase. They are quite common, and any fracture through a 5 mm × 2 mm section will show several. The director field associated with the feature is consistent with that of a point defect with α close to 120°. It is also pertinent to note that this angle of 'swirl' corresponds to a point defect with minimum splay distortion (see figure 5). Of all the possible point geometries considered, this is the one which would be energetically favoured in liquid crystalline phases of polymers which have a splay constant which is high compared with that of bend or twist. While this comparison is nice, it is important to enquire whether the structures observed really do represent isolated point singularities, as it is possible that the features such as that in figure 6 are sections through line defects. However, the presence of an $s = 1$ line defect in a nematic phase can be questioned on two counts, firstly that it is topologically unstable, tending to escape in the third dimension [16, 20, 21], and secondly, that it is energetically unstable and thus capable of lowering its energy by splitting into two lines each of strength $\frac{1}{2}$ [22]. The second possibility is not observed, but there are reasons to suppose that when the splay energy is uniquely high, the tendency to split is much reduced, even absent altogether [10]. As observed, the defects give little indication of an escaped structure; the directors appear to lie in a plane in the central region rather than seeking parallelism by escaping into the 'third' dimension. It is very possible that the fracture path is selectively intersecting an escaped $s = 1$ disclination at the site of point defects along its axis, but we need further experimental evidence before we can be sure on this point.

4. Summary

(i) A point singularity can be usefully described in terms of a transforming disclination loop in which the rotation vector, Ω, of the disclination maintains a constant angle, α, with the line. The loop effects the transformation from a monodomain (inside loop) to a point field (outside), and its collapse generates a point singularity. The angle α characterizes the point.

(ii) The total energies of the points (excluding surface energies) have been calculated as a function of kR, for all values of α. The splay contribution is highest for $\alpha = 0°$ (*noeud*) and lowest for $\alpha = 115°$ (*col-foyer* range). Twist is greatest at $\alpha = 90°$ (centre) and zero at both the *noeud* and *col* extremes, while bend is zero for the *neoud* and a maximum at $\alpha = 105°$.

(iii) Fractography of bulk samples of a quenched main chain liquid crystalline polymer shows defect geometries which are consistent with $\alpha \approx 115°$ point singularities. Such singularities will be preferred in nematic polymers on account of the high splay energy associated with the long molecules.

The authors wish to acknowledge stimulating discussions with Prof. S. Chandrasekhar, Prof. M. Kléman, Dr E. M. Terentjev, and members of the Isaac Newton Institute for Mathematical Sciences in Cambridge. This work was carried out as a part of an EPSRC programme.

References

[1] Reinitzer, F., 1988, *Monatsch*, **9,** 421.
[2] Poincaré, H., 1886, *J. de Math.*, **2,** 151.
[3] Nabarro, F. R. N., 1972, *J. de Phys.*, **33,** 1089.
[4] Frank, F. C., 1958, *Discuss. Faraday Soc.*, **25,** 19.
[5] Meyer, R. B., 1982, *Polymer Liquid Crystals*, edited by R. B. Meyer, W. R. Krigbaum and A. Ciferri (Academic Press), 133–164.
[6] Donald, A. M., and Windle, A. H., 1992, *Liquid Crystalline Polymers* (C.U.P.).
[7] Volovik, G. E., and Lavrentovich, O. D., 1983, *Soviet Phys. JETP*, **58,** 1159.
[8] Kléman, M., 1973, *Phil. Mag.*, **27,** 1057.
[9] Press, M. J., and Arrott, A. S., 1975, *J. de Phys. Colloque C1*, **36,** 177.
[10] Windle, A. H., Assender, H. E., and Lavine, M. S., 1994, *Phil. Trans. Royal Soc. Lond.*, **348,** 73.
[11] Dubois-Violette, E., and Parodi, O., 1969, *J. de Phys.*, **30,** C4-57.
[12] Kurik, M. V., Levrentovich, O. D., 1988, *Soviet Phys. Usp.*, **31,** 196.
[13] Hearn, A. C., 1991, REDUCE 3.4 (RAND Corporation).
[14] Chuang, I., Durrer, R., Turok, N., and Yurke, B., 1991, *Science*, **251,** 1336.
[15] Kléman, M., 1991, *Phase Transitions*, **30,** 217.
[16] Williams, C., Pieranski, O., and Cladis, P. E., 1972, *Phys. Rev. Lett.*, **29,** 90.
[17] Melzer, D., and Nabarro, F. R. N., 1977, *Phil. Mag.*, **35,** 901.
[18] Melzer, D., and Nabarro, F. R. N., 1977, *Phil. Mag.*, **35,** 907.
[19] Lavrentovich, O. D., and Terentjev, E. M., 1986, *Soviet Phys. JETP*, **64,** 1237.
[20] Meyer, R. B., 1973, *Phil. Mag.*, 27, 405.
[21] Cladis, P. E., and Kléman, M., 1972, *J. de Phys.*, **33,** 591.
[22] Nehring, J., and Saupe, A., 1972, *J. chem. Soc. Faraday Trans. II*, **68,** 1.